

# Effects of cation $d$ states on the structural and electronic properties of III-nitride and II-oxide wide-band-gap semiconductors

Anderson Janotti, David Segev, and Chris G. Van de Walle  
*Materials Department, University of California, Santa Barbara, CA 93106-5050, USA*  
 (Received 18 August 2005; published 11 July 2006)

Using first-principles methods based on density functional theory within the local density approximation (LDA) we calculate the structural and electronic properties of wurtzite MgO, ZnO, and CdO, and discuss their similarities and dissimilarities with the corresponding Group-III nitrides AlN, GaN, and InN. We treat the semicore  $d$  states of Zn, Cd, Ga, and In explicitly as valence states in a pseudopotential approach, investigate the effects of including on-site Coulomb interaction for Zn, Cd, Ga, and In semicore  $d$  states within the LDA+ $U$  method, and propose a novel approach to calculate the parameter  $U$ . Our results show that the LDA+ $U$  approach systematically improves the LDA band gap by indirectly acting on both the valence-band maximum and conduction-band minimum. We also discuss the effects of the on-site Coulomb interaction on structural parameters and absolute deformation potentials of ZnO, CdO, GaN, and InN.

DOI: [10.1103/PhysRevB.74.045202](https://doi.org/10.1103/PhysRevB.74.045202)

PACS number(s): 71.15.Mb, 71.20.Nr

## I. INTRODUCTION

Parallel to the nitride semiconductors, which have emerged as leading materials for optoelectronic device applications spanning the ultraviolet and visible region of the spectrum, there is growing interest in ZnO and direct band-gap  $\text{Cd}_y\text{Mg}_x\text{Zn}_{1-x-y}\text{O}$  alloys.<sup>1-4</sup> ZnO is a wide-band-gap semiconductor with unique piezoelectric, optical, and electronic properties. It is available in large single crystals, with a direct band gap (3.4 eV) and a large exciton binding energy (60 meV).<sup>5,6</sup> Adding Cd to ZnO decreases the band gap, whereas adding Mg increases the band gap. For modest Cd or Mg concentrations, MgZnO and CdZnO alloys assume the wurtzite structure,<sup>2-4</sup> in spite of the fact that MgO and CdO occur in the rocksalt structure. Since no experimental data are available for MgO or CdO in the wurtzite structure, the commonly used approach of interpolating between the binary compounds to obtain alloy properties is not possible. This is our motivation for performing a computational study of the structural and electronic properties of MgO and CdO in the wurtzite phase. The results will also allow us to conduct a systematic analysis of the similarities and dissimilarities between the oxides MgO, ZnO, CdO, and the corresponding nitrides AlN, GaN, and InN.

In both the nitrides (GaN and InN) and the oxides (ZnO and CdO) semicore cation  $d$  states potentially play an important role. In the nitrides, the cation  $d$  states lie near the bottom of the valence band and hybridize with those states, which are comprised mainly of N  $2s$  states. In the oxides, on the other hand, the cation  $d$  states lie near the middle of the valence band. In both cases the  $d$  states interact and hybridize with the states at the valence-band maximum, which are comprised mostly of anion  $2p$  states. The  $p$ - $d$  coupling shifts up the valence-band maximum and is thus expected to affect band lineups.<sup>7,8</sup> In particular, the effect of the  $d$  electrons on the valence-band lineup should manifest itself when comparing nearly lattice-matched compounds such as MgO and ZnO, where the  $d$  electrons are absent on the MgO side and influential on the ZnO side. Since the magnitude of the coupling is increased when the crystal is compressed, it is also

expected to affect the pressure coefficient (i.e., the deformation potential) of the valence band.

Density functional theory (DFT) within the local density approximation (LDA)<sup>9</sup> is by now the standard approach for calculating the electronic and structural properties that are the focus of the present investigation. Yet it is well known that DFT-LDA underestimates band gaps of semiconductors and insulators. This deficiency of DFT-LDA has been widely discussed in the past, and it has been attributed largely to discontinuities in the derivative of the exchange-correlation energy.<sup>10-12</sup> Unfortunately DFT-LDA also underestimates the binding energy of the semicore  $d$  states and consequently overestimates their hybridization with the anion  $p$ -derived valence states, enhancing the effects of the  $p$ - $d$  coupling. The artificially large  $p$ - $d$  coupling pushes up the valence-band maximum, leading to a further reduction in the calculated band gap. In the case of CdO and InN, a closing of the band gap is observed, predicting a qualitatively wrong metallic ground state. Applying the generalized gradient approximation instead of the LDA does not alleviate these problems.<sup>13</sup> Even performing quasiparticle calculations using the GW approximation does not correct for the incorrect positioning of the  $d$  states, if the standard approach is followed of taking DFT wave functions as the starting point of the GW calculations.<sup>14</sup> Other potential corrections that have been discussed include model GW calculations,<sup>15</sup> an artificially increased LDA exchange-potential coefficient,<sup>16</sup> and screened differences in self-consistent-field calculations ( $\Delta\text{SCF}$ ) for atoms.<sup>17</sup>

In this paper we report calculations based on the LDA+ $U$  method.<sup>18-21</sup> The on-site Coulomb interaction  $U$  accounts for strong electronic interactions in narrow bands composed of spatially localized atomic-like states ( $l=2,3$ ). These strong Coulomb interactions are not adequately described in DFT-LDA, and the LDA+ $U$  approach aims to correct for this by adding an orbital-dependent term to the LDA potential. An important issue within the LDA+ $U$  approach is the choice of the parameter  $U$ , for which no rigorous prescription exists. One approach is to derive  $U$  from calculations for the solid; among the methods that have been

proposed are constrained LDA calculations<sup>18–22</sup> and linear response calculations.<sup>23</sup> These methods tend to be computationally cumbersome, and while in principle based on first principles, necessarily involve various approximations. Approaches that were designed to be applied within a linearized muffin-tin orbital or augmented plane wave methods are also not transferrable to pseudopotential methods. Another approach for choosing  $U$  has relied on adjusting the parameter to reproduce experimental photoemission results.<sup>24</sup> However, this procedure does not take into account the effect of the core-hole final state, and thus overestimates the magnitude of the correction. Here we propose a systematic and general approach to calculate the on-site Coulomb interaction parameter  $U$ , based on first-principles atomic calculations. We illustrate our approach with calculations of the basic structural and electronic properties of ZnO, CdO, GaN, and InN, focusing on a comparison between LDA and LDA+ $U$  results.

The paper is organized as follows. First we describe the theoretical methods and the procedure for calculating the on-site Coulomb interaction parameter  $U$ . Then, in Sec. III A we report results for the structural properties of the oxides MgO, ZnO, CdO and the nitrides AlN, GaN, InN, and the effect of  $U$  on these properties. In Sec. III B we discuss the effects of  $U$  on the single-particle electronic band structures. In particular, we investigate how  $U$  affects the position of valence band and conduction band edges separately. In Sec. III C we discuss the effects of  $U$  on the absolute deformation potentials. Section IV summarizes our results.

## II. METHODS

The calculations were performed using the pseudopotential method with the projector augmented wave potentials as implemented in the VASP code.<sup>25,26</sup> We use an energy cutoff of 500 eV for the plane-wave basis set expansion and a  $4 \times 4 \times 4$  set of special  $k$  points for the integrations over the Brillouin zone of the wurtzite structure with four atoms per primitive cell. The LDA typically gives lattice constants within 2% of the experimental values, but it severely underestimates electronic band gaps. In the case of semiconductors with cation semicore  $d$  states, the error is particularly severe because the LDA underestimates the binding energy of the  $d$  states, and therefore overestimates their hybridization with the anion- $p$  valence states, amplifying the effects of the  $p$ - $d$  coupling, as discussed above. In this paper we use the LDA+ $U$  method to overcome this deficiency in the case of ZnO, CdO, GaN, and InN. We propose a method to calculate the on-site Coulomb interaction parameter from first principles. Our actual implementation involves an approximation, but in principle our entire approach for calculating  $U$  could be implemented without relying on any input from experiment.

In the LDA+ $U$  approach one separates the valence electrons in two subsystems: localized  $d$  or  $f$  electrons for which Coulomb  $d$ - $d$  (or  $f$ - $f$ ) interactions should be taken into account via a Hubbard-like Hamiltonian, and delocalized  $s$  and  $p$  electrons for which the LDA description based on orbital-independent one-electron potentials is sufficient.<sup>18,19</sup> In the rotationally invariant form of the LDA+ $U$  by Liechtenstein *et al.*,<sup>20,21</sup> the total energy is given by

$$E_{\text{tot}}^{\text{LDA}+U}[\rho(\mathbf{r}), \{n\}] = E_{\text{tot}}^{\text{LDA}}[\rho(\mathbf{r})] + E^U(\{n\}) - E_{\text{dc}}(\{n\}), \quad (1)$$

with the added on-site Coulomb interaction  $E^U(\{n\})$  given by a Hartree-Fock-like interaction,

$$E^U(\{n\}) = \frac{1}{2} \sum_{t, \sigma, \sigma'} \sum_{\alpha, \beta, \gamma, \delta} \langle \chi_{\alpha}^t, \chi_{\gamma}^t | V_{ee} | \chi_{\beta}^t, \chi_{\delta}^t \rangle n_{\alpha, \beta}^{t, \sigma} n_{\gamma, \delta}^{t, \sigma'} - \frac{1}{2} \sum_{t, \sigma} \sum_{\alpha, \beta, \gamma, \delta} \langle \chi_{\alpha}^t, \chi_{\gamma}^t | V_{ee} | \chi_{\beta}^t, \chi_{\delta}^t \rangle n_{\alpha, \beta}^{t, \sigma} n_{\gamma, \delta}^{t, \sigma}. \quad (2)$$

The first summation is over all sites  $t$  containing the localized valence electrons (semicore  $d$  electrons in our case) and each spin direction  $\sigma$ ; the elements  $n_{\alpha, \beta}^{t, \sigma}$  of the occupation matrix  $\{n\}$  are obtained by projecting the crystal wave functions  $\Psi_{n, \mathbf{k}}$  onto atomic orbitals inside the augmentation region:<sup>27</sup>

$$n_{\alpha, \beta}^{t, \sigma} = \sum_{n, \mathbf{k}} f_{n, \mathbf{k}}^{\sigma} \langle \Psi_{n, \mathbf{k}}^{\sigma} | P_{\alpha, \beta}^t | \Psi_{n, \mathbf{k}}^{\sigma} \rangle, \quad (3)$$

where  $f_{n, \mathbf{k}}$  is the occupation of the  $\Psi_{n, \mathbf{k}}$  Bloch state, and  $P_{\alpha, \beta}^t$  are the projection operators ( $P_{\alpha, \beta}^t = |l m_{\alpha}\rangle \langle l m_{\beta}|$  inside the augmentation region, and 0 otherwise).

The matrix elements  $\langle \chi_{\alpha}^t, \chi_{\gamma}^t | V_{ee}^e | \chi_{\beta}^t, \chi_{\delta}^t \rangle$  are the four-center matrix elements of the screened Coulomb interaction  $V_{ee}$  between ( $d$  or  $f$ ) electrons sitting on the same site. Dropping the site index  $t$  for writing convenience, these matrix elements are defined in terms of radial Slater integrals  $F^k$  ( $k=0, 1, 2, \dots$ )<sup>27</sup> as

$$\langle \chi_{\alpha}, \chi_{\gamma} | V_{ee} | \chi_{\beta}, \chi_{\delta} \rangle = \sum_k a_k(\alpha, \beta, \gamma, \delta) F^k, \quad (4)$$

with

$$a_k(\alpha, \beta, \gamma, \delta) = \frac{4\pi}{2k+1} \sum_{q=-k}^{q=k} \langle l m_{\alpha} | Y_{kq} | l m_{\beta} \rangle \langle l m_{\gamma} | Y_{kq}^* | l m_{\delta} \rangle, \quad (5)$$

where ( $l m_{\alpha}$ ) are the angular momenta quantum numbers of  $|\chi_{\alpha}\rangle$ . For  $d$  electrons ( $l=2$ ), only  $F^0$ ,  $F^2$ , and  $F^4$  contribute to the sum in Eq. (4), and the effective on-site Coulomb and exchange parameters  $U$  and  $J$  are related to the radial Slater integrals  $F^k$  via  $U=F^0$  and  $J=(F^2+F^4)/14$ .

The term  $E_{\text{dc}}(\{n\})$  that corrects for the double counting of the electron-electron Coulomb interaction is given by

$$E_{\text{dc}}(\{n\}) = \sum_t \left\{ \frac{U}{2} \sum_{\sigma, \sigma'} N^{t, \sigma} (N^{t, \sigma'} - \delta_{\sigma, \sigma'}) - \frac{J}{2} \sum_{\sigma} N^{t, \sigma} (N^{t, \sigma} - 1) \right\}, \quad (6)$$

with  $N^{t, \sigma} = \sum_{\alpha} n_{\alpha, \alpha}^{t, \sigma}$ .

Here we neglect the effects associated with higher-multipolar terms in the Coulomb interaction and the differences between the Coulomb interactions in spin-up and spin-down channels by setting the effective exchange splitting parameter to  $J=0$ . In this case, the only nonvanishing term in the sum of Eq. (4) is for  $k=0$ , and one can see from Eq. (5)

that  $a_0(\alpha, \beta, \gamma, \delta) = \delta_{\alpha\beta}\delta_{\gamma\delta}$ . Therefore, we can simplify the added Hartree-Fock-like term  $E^U(\{n\})$  and rewrite Eq. (2) in the form

$$E^U(\{n\}) = \frac{U}{2} \sum_t \left\{ \sum_{\alpha, \beta, \sigma, \sigma'} n_{\alpha, \alpha}^{t, \sigma} n_{\beta, \beta}^{t, \sigma'} - \frac{1}{2} \sum_{\alpha, \beta, \sigma} n_{\alpha, \beta}^{t, \sigma} n_{\beta, \alpha}^{t, \sigma} \right\}. \quad (7)$$

It is also instructive to write the double-counting term  $E_{dc}(\{n\})$  [Eq. (6)] explicitly in terms of the matrix elements  $n_{\alpha, \alpha}^{t, \sigma}$ .

$$E_{dc}(\{n\}) = \frac{U}{2} \sum_t \left\{ \sum_{\alpha, \beta, \sigma, \sigma'} n_{\alpha, \alpha}^{t, \sigma} n_{\beta, \beta}^{t, \sigma'} - \sum_{\alpha, \sigma} n_{\alpha, \alpha}^{t, \sigma} \right\}. \quad (8)$$

It is interesting to note that the term  $E^U(\{n\})$  [Eq. (7)] that has been added to the LDA total energy  $E_{\text{tot}}^{\text{LDA}}$  in Eq. (1) is self-interaction free because terms like  $n_{\alpha, \alpha}^{t, \sigma} n_{\alpha, \alpha}^{t, \sigma}$  cancel out on the right-hand side of Eq. (7). Equation (8) clearly shows these self-interaction terms such as  $n_{\alpha, \alpha}^{t, \sigma} n_{\alpha, \alpha}^{t, \sigma}$  have been subtracted from the LDA total energy  $E_{\text{tot}}^{\text{LDA}}$ . Hence, we can write the total energy in the LDA+ $U$  approach as

$$E_{\text{tot}}^{\text{LDA}+U}[\rho(\mathbf{r}), \{n\}] = E_{\text{tot}}^{\text{LDA}}[\rho(\mathbf{r})] + \sum_t \frac{U}{2} \left\{ \sum_{\alpha, \sigma} n_{\alpha, \alpha}^{t, \sigma} - \sum_{\alpha, \beta, \sigma} n_{\alpha, \beta}^{t, \sigma} n_{\beta, \alpha}^{t, \sigma} \right\}. \quad (9)$$

The LDA+ $U$  method was originally conceived for, and has most often been applied to, systems with strongly interacting electrons in *partially filled* bands.<sup>18–23</sup> Here we apply LDA+ $U$  to *completely filled* bands composed of semicore states in wide-band gap semiconductors. The strong electron-electron interaction in these narrow bands composed of semicore  $d$  states is also poorly described by the local density approximation. Indeed, we do not expect electron-electron interactions in narrow bands originating from spatially localized atomic-like states to be well described by a homogeneous electron gas. This description can be improved by following the LDA+ $U$  procedure of subtracting an “effective” LDA Coulomb interaction (given by the  $E_{dc}(\{n\})$ ) from the LDA total energy  $E_{\text{tot}}^{\text{LDA}}$ , and adding back a Hartree-Fock-like interaction term  $E^U(\{n\})$ . From the expression for the total energy in the LDA+ $U$  approach [Eq. (9) above], we can expect the Kohn-Sham energies (in the LDA+ $U$ ) associated with narrow bands derived from atomic-like states to be shifted with respect to their respective LDA energies according to

$$\varepsilon_{\alpha}^{\text{LDA}+U} = \frac{\partial E_{\text{tot}}^{\text{LDA}+U}}{\partial n_{\alpha, \alpha}} = \varepsilon_{\alpha}^{\text{LDA}} + U \left( \frac{1}{2} - n_{\alpha, \alpha} \right). \quad (10)$$

Therefore, the net effect of the added on-site Coulomb interaction is to shift these fully occupied narrow  $d$  bands down in energy by  $\sim U/2$  with respect to the other bands (for which the LDA provides an adequate description).

It is appropriate to comment on similarities and differences between the LDA+ $U$  approach and the self-interaction correction (SIC) method.<sup>28,29</sup> The SIC is intended to correct

for the spurious self-interaction intrinsic to the Kohn-Sham approach, where each electron interacts with itself via the electrostatic Coulomb energy. This nonphysical interaction would be cancelled by a contribution from the exchange energy in an exact formalism. Although conceptually different from the SIC, the LDA+ $U$  produces effects very similar to SIC when applied to strongly interacting electrons in completely filled bands, since it treats the interactions in a Hartree-Fock-like approach as discussed above. We note that SIC implementations tend to be much more computationally involved.<sup>29</sup>

The choice of the  $U$  parameter is obviously crucial if one expects the LDA+ $U$  approach to lead to improvements over the LDA description for real systems. Here we propose a specific method to calculate the on-site Coulomb interaction parameter  $U$  from first principles.  $U$  is defined as the Coulomb energy interaction between the  $d$  electrons on the same atom. We obtain an *atomic* correlation energy  $U^{\text{at}}$  as the energy difference between the addition and the removal of an electron from the atomic  $d$  subshell:

$$U^{\text{at}} = [E_{\text{tot}}(d^{m+1}) - E_{\text{tot}}(d^m)] - [E_{\text{tot}}(d^m) - E_{\text{tot}}(d^{m-1})], \quad (11)$$

where  $E_{\text{tot}}(d^m)$  is the total energy of the isolated atom with  $n$  electrons occupying the  $d$  subshell ( $l=2$ ). Because the atomic  $d$  subshells of Zn, Cd, Ga, and In are completely filled, the  $d^9$  configuration is taken as the reference ( $n=9$ ). Since the atomic wave functions are more localized in the  $d^9$  configuration compared to the  $d^{10}$  configuration, this approximation will tend to overestimate the value of  $U^{\text{at}}$  by  $\sim 1$  eV. However, when divided by the dielectric constant (see the following), the error in the effective  $U$  used in the calculations for the solid is quite small, and this error does not affect our main conclusions.

When the atoms are assembled in a solid, the atomic Coulomb correlation interaction is screened by the optical dielectric constant  $\varepsilon^{\infty}$ , leading to an effective on-site Coulomb correlation interaction  $U = U^{\text{at}}/\varepsilon^{\infty}$ . In principle one could use experimental values for  $\varepsilon^{\infty}$ , but for the purpose of the present study we again encounter the problem that no values are available for CdO in the wurtzite structure. We therefore calculate the optical dielectric constants using linear response,<sup>30</sup> as implemented in the ABINIT code.<sup>31</sup> The optical dielectric constant is particularly sensitive to the band gap of the material; in the calculation of  $\varepsilon^{\infty}$  we therefore use a “scissors operator”<sup>33</sup> to correct the band gap of ZnO, CdO, GaN, and InN. In the case of CdO, the band-gap correction is taken from rocksalt CdO, and we assume the same shift applies to the wurtzite phase. Note that instead of using a scissors operator, one could in principle carry out quasiparticle calculations in the GW approximation,<sup>32</sup> rendering the entire approach first-principles, without any input from experiment. However, since the use of the scissors operator is known to produce good results for calculating dielectric constants<sup>33</sup> (which we verified in cases that could be directly compared with experiment, as demonstrated in the following), we thought it justified to avoid the arduous task of performing

TABLE I. Calculated optical dielectric constants  $\epsilon^\infty$  for AlN, GaN, InN, MgO (wurtzite), MgO (rocksalt), ZnO, CdO (wurtzite), and CdO (rocksalt) using the scissors operator as described in the text. Experimental values (Refs. 6, 34, and 35) are listed where available. The values for the wurtzite phase represent the weighted average between  $\epsilon_\perp^\infty$  and  $\epsilon_\parallel^\infty$ .

	Theory	Experiment
AlN	3.9	4.8
GaN	5.0	5.2
InN	7.6	8.4
MgO (wurtzite)	2.6	...
MgO (rocksalt)	2.7	2.9
ZnO	3.8	3.7
CdO (wurtzite)	6.7	...
CdO (rocksalt)	5.9	6.2

the full GW calculations and to rely on the scissors-operator approximation.

The calculated dielectric constants  $\epsilon^\infty$  for the oxides MgO, ZnO, CdO, and nitrides AlN, GaN, and InN are listed in Table I. We note that the calculated dielectric constants  $\epsilon^\infty$  are in good agreement with the experimental values<sup>6,34,35</sup> where available. For MgO the calculated  $\epsilon^\infty$  for the wurtzite phase is 2.6, while that for the rocksalt phase is 2.7, and the experimental value for the rocksalt phase is 2.9. For CdO the calculated  $\epsilon^\infty$  for the wurtzite phase is 6.5, while that for the rocksalt phase is 5.9, and the experimental value for the rocksalt phase is 6.2.

In Table II we list the calculated values of the dielectric constants  $\epsilon^\infty$ , the atomic Coulomb correlation energy  $U^{\text{at}}$  for the  $d$  states, and the effective (screened)  $U$  used in the LDA+ $U$  calculations. The values reported here for  $\epsilon^\infty$  are the weighted average of the calculated components of the optical dielectric tensor perpendicular and parallel to the  $c$  axis,  $\epsilon_\perp^\infty$  and  $\epsilon_\parallel^\infty$ . Table II shows that the on-site Coulomb correlation energies  $U$  for  $4d$  electrons (CdO, InN) are significantly smaller than those for  $3d$  electrons (ZnO, GaN), corresponding to the smaller degree of localization and enhanced screening experienced by the  $4d$  states. Combined with the fact that  $\epsilon^\infty$  is *larger* in CdO and InN, this leads to significantly smaller values of  $U$  in these compounds.

As mentioned in Sec. I, alternative first-principles approaches for obtaining the parameter  $U$  exist;<sup>21,22</sup> however, they tend to be more computationally intensive, not easy to implement in a pseudopotential approach, and also involve

TABLE II. Calculated dielectric constant, atomic electron correlation energy  $U^{\text{at}}$  for Zn, Cd, Ga, and In, and the on-site Coulomb interaction energy  $U=U^{\text{at}}/\epsilon^\infty$  for ZnO, CdO, GaN, and InN.

	$U^{\text{at}}$ (eV)	$\epsilon^\infty$	$U$ (eV)
ZnO	18.0	3.8	4.7
CdO	13.8	6.7	2.1
GaN	19.6	5.0	3.9
InN	14.4	7.6	1.9

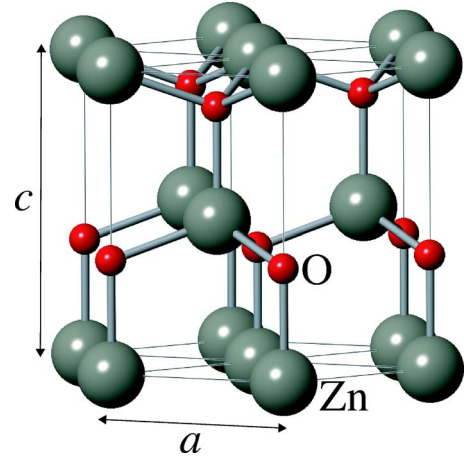


FIG. 1. (Color online) Ball and stick model of the wurtzite structure. The external lattice parameters  $a$  and  $c$  are indicated. The internal structural parameter  $u$  is defined as the length of the bond parallel to the  $c$  axis, in units of  $c$ .

approximations. Since the alternative approaches rely on different computational techniques and have been applied to very different materials systems, a detailed comparison is beyond the scope of this paper. We do want to emphasize the simplicity and relatively modest computational effort of the method presented here.

### III. RESULTS

#### A. Structural lattice parameters

The wurtzite structure contains two formula units per primitive unit cell and can be described by the lattice constants  $a$  and  $c$ , and the dimensionless internal structural parameter  $u$ .  $u$  is defined as the length of the bond parallel to the  $c$  axis, in units of  $c$ , as shown in Fig. 1. In the ideal wurtzite structure,  $c/a=1.6333$  and  $u=0.375$ . In Table III we list the calculated equilibrium structural parameters of wurtzite MgO, ZnO, CdO, and, for comparison, AlN, GaN, and InN. First, we note that the calculated LDA values for ZnO, AlN, GaN, and InN agree with the experimental values within better than 2%. For MgO and CdO in the rocksalt ground-state structure, the calculated LDA lattice constants are  $a=4.151$  Å and  $a=4.662$  Å, in good agreement with the experimental values of 4.216 and 4.689 Å, respectively.<sup>6</sup> Hence, we expect that the structural parameters of wurtzite MgO and CdO, where experimental data are not available, are described with similar accuracy by the LDA approximation. As such, we predict a small in-plane lattice mismatch of less than +2% between wurtzite MgO and ZnO, and a large in-plane lattice mismatch of about +12% between wurtzite CdO and ZnO. Similar mismatches are also observed in nitrides, i.e., -2% between AlN and GaN, and +11% between InN and GaN.

Note that the axial ratio  $c/a$  and the internal parameter  $u$  for wurtzite MgO exhibit the largest departures from the ideal wurtzite values. We find  $c/a=1.512$  and  $u=0.398$ . We also find wurtzite MgO to be stable against small variations of  $c/a$  and  $u$  around the calculated equilibrium values. How-

TABLE III. Calculated lattice constants  $a$  and  $c/a$  and internal structural parameter  $u$  of MgO, ZnO, CdO, AlN, GaN, and InN in the wurtzite phase. Experimental data are listed where available (Refs. 6 and 38).

Compound	$a$ (Å)			$c/a$			$u$		
	LDA	LDA+ $U$	Expt	LDA	LDA+ $U$	Expt	LDA	LDA+ $U$	Expt
MgO	3.261			1.514			0.398		
ZnO	3.195	3.148	3.249	1.615	1.612	1.602	0.379	0.379	0.382
CdO	3.589	3.488		1.564	1.563		0.389	0.389	
AlN	3.090		3.111	1.602		1.600	0.382		0.382
GaN	3.152	3.094	3.190	1.631	1.629	1.627	0.376	0.377	0.377
InN	3.507	3.488	3.545	1.618	1.617	1.609	0.379	0.379	0.375

ever, we note that for large values of  $u$  ( $u > 0.42$ ) the system spontaneously relaxes to the  $h$ -MgO structure with  $c/a = 1.199$  and  $u = 0.5$ , as previously reported.<sup>36,37</sup> In order to verify the local stability of the wurtzite structure in  $Zn_{1-x}Mg_xO$  alloys, we performed calculations for ordered alloys with  $x = 0.125, 0.25$ , and  $0.375$ . We found that the wurtzite local atomic geometry is stable against displacements of the Mg atom along the  $c$  direction, and Mg remains fourfold coordinated. MgZnO alloys with modest amounts of Mg will therefore *not* display the three-folded coordination characteristic of  $h$ -MgO.

We also note from Table III that the LDA+ $U$  method systematically gives smaller lattice constants than the LDA. This is due to the fact that the application of  $U$  causes the  $d$  states to become more localized, and therefore results in smaller lattice constants. This is consistent with the observation that, in the extreme case of pseudopotentials with the  $d$  states in the core, the calculated lattice constants of II-VI compounds are much too small compared to the experimental value.<sup>7</sup>

### B. Electronic band structure

In Fig. 2 we show the calculated LDA single-particle band structure for MgO and CdO in the rocksalt and wurtzite structures. The calculated band gaps are listed in Table IV. The band gap is direct for both rocksalt and wurtzite MgO. The calculated LDA band gap for rocksalt MgO is 5.1 eV. Comparing with the experimental value of 7.9 eV<sup>6</sup> shows that the LDA error is 2.8 eV, or more than 30% of the experimental gap, which is typical of LDA. Our calculations show that the LDA band gap of wurtzite MgO is 3.6 eV, i.e., 1.5 eV smaller than that of rocksalt MgO. If we assume that the LDA error is the same for rocksalt and wurtzite structures we can predict a band gap of 6.4 eV for wurtzite MgO.

In the case of CdO, we find a metallic ground state for both rocksalt and wurtzite structures due to the LDA band-gap error. Nevertheless, LDA does correctly predict an “indirect” band gap for the rocksalt phase, where the valence-band maximum occurs at the  $L$  point and the conduction-band minimum occurs at the  $\Gamma$  point [see Fig. 2(b)]. For wurtzite CdO we find a direct band gap, with the valence-band maximum and conduction-band minimum both at  $\Gamma$ . We calculate  $E_g = -0.45$  eV for rocksalt CdO and  $E_g$

$= -0.34$  eV for wurtzite CdO. Experimental values of the indirect band gap  $E_g(L-\Gamma)$  of rocksalt CdO vary over a wide range, from 0.8 to 1.2 eV, the variations being attributed to the Moss-Burstein effect<sup>6,39,40</sup> and the difficulty in controlling doping. For this reason we focus on the less controversial value of the direct band gap at  $\Gamma$  for comparisons. We find  $E_g(\Gamma-\Gamma) = 1.04$  eV compared to the experimental value of 2.28 eV, a LDA error of 1.24 eV. Assuming the LDA error to be the same for  $E_g(L-\Gamma)$  as it is for  $E_g(\Gamma-\Gamma)$ , the indirect band gap of rocksalt CdO becomes  $E_g(L-\Gamma) = 0.79$  eV, consistent with the lower end of the range of reported experimental values. For wurtzite CdO, applying the same correction yields  $E_g = 0.90$  eV for the direct band gap at  $\Gamma$ .

We now investigate the effects of the position of the  $d$  states on the calculated band gaps. In Fig. 3 we show the calculated single-particle band structures of wurtzite ZnO, CdO, GaN, and InN using the LDA and LDA+ $U$  approximations. We find that the LDA+ $U$  systematically improves the LDA band gap. For ZnO we find  $E_g = 1.51$  eV using LDA+ $U$ , compared to  $E_g = 0.80$  eV using the LDA, but still

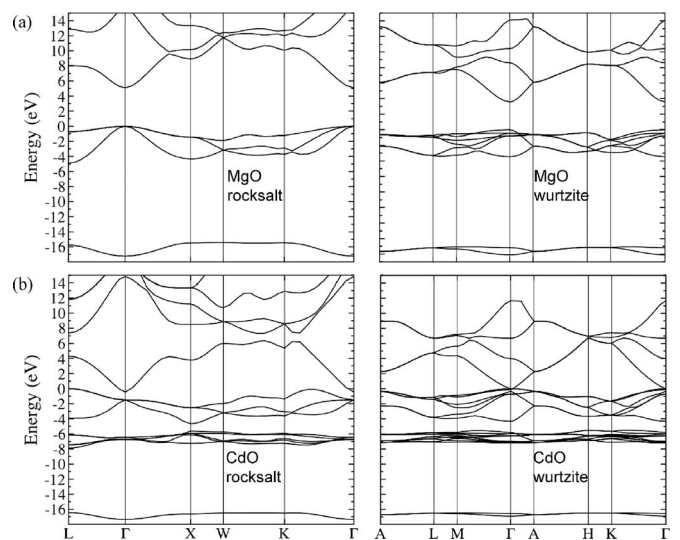


FIG. 2. Calculated LDA electronic band structures of (a) MgO and (b) CdO in the ground-state rocksalt structure (left) and the wurtzite structure (right). The zero of energy was placed at the respective valence-band maximum  $E_v$ .

TABLE IV. Calculated band gaps [ $E_g(\Gamma-\Gamma)$ ] for AlN, GaN, InN, MgO (wurtzite), MgO (rocksalt), ZnO, CdO (wurtzite), and CdO (rocksalt) using the LDA and LDA+ $U$  approximations. Experimental values are listed where available (Refs. 6 and 41). The values with an asterisk represent the predicted band gap based on the difference between the calculated band gaps of rocksalt and wurtzite phases.

	LDA	LDA+ $U$	Expt.
AlN	4.41	...	6.19
GaN	2.14	2.87	3.50
InN	-0.18	0.03	0.7-0.8
MgO (rocksalt)	5.09	...	7.9
MgO (wurtzite)	3.58	...	6.4*
ZnO	0.80	1.51	3.43
CdO (rocksalt)	1.04	1.16	2.28
CdO (wurtzite)	-0.34	-0.20	0.92*

much lower than the experimental value of 3.43 eV.<sup>6</sup> For rocksalt CdO, using the LDA+ $U$ , we find  $E_g(\Gamma-\Gamma) = 1.16$  eV, an error of 1.12 eV. For wurtzite CdO, we find  $E_g = -0.20$  eV using LDA+ $U$ . Adding the band-gap error, the predicted band gap of wurtzite CdO is  $E_g = 0.92$  eV, consistent with the prediction based on the LDA values.

Similar improvements in the band gap are also observed for GaN and InN by including on-site Coulomb correlation interaction in the LDA+ $U$  method, although the  $d$  states are now near the bottom of the valence band, more than 12 eV below the valence-band maximum. The LDA+ $U$  band gap is 2.87 eV for GaN, compared to the LDA value of 2.14 eV; for InN, LDA+ $U$  gives 0.03 eV compared to -0.18 eV in LDA.

Figure 3 shows a quantitative change in the position of the single-particle  $d$  states going from the LDA to the LDA+ $U$  approximation. The  $d$  states are pushed down by more than 1 eV with respect to the valence-band maximum, consistent with the increased localization of these states. The largest corrections occur for ZnO and GaN, due to the more localized nature of the  $d$  states compared to CdO and InN, where the  $4d$  states are more efficiently screened by the Cd and In core electrons.

It is important to stress that one should *not* expect the inclusion of on-site Coulomb correlation interactions to completely heal the LDA deficiency in underestimating band gaps. Indeed, the usual LDA band-gap problem arising from a discontinuity in the exchange and correlation potential<sup>10-12</sup> is obviously still present, and not addressed by the LDA+ $U$  treatment. The band gap involves transitions between the top of the valence band (derived mostly from the anion  $p$  valence states) and the bottom of the conduction band (derived mostly from cation  $s$  valence states). These are extended Bloch states to which the on-site Coulomb interaction  $U$  is not directly applied, and they are treated here within the LDA. Still, we observe that correcting the position of the cation  $d$  states causes a systematic improvement in the band gap in both oxides and nitrides. More important, the correction imparted by the LDA+ $U$  treatment reflects a specific

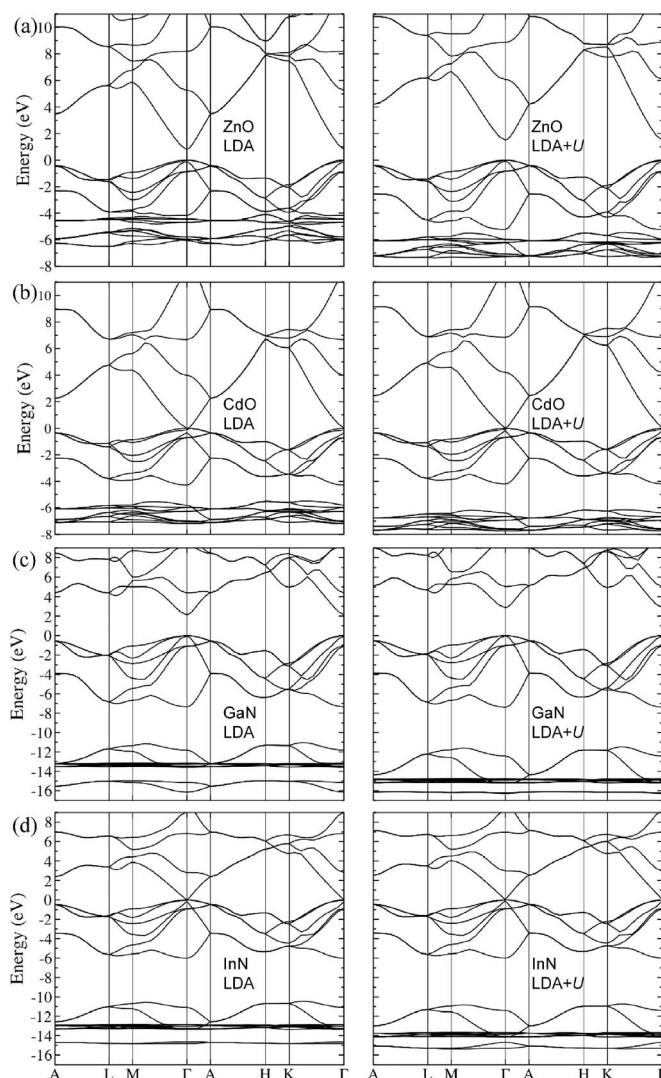


FIG. 3. Calculated single-particle electronic band structures of (a) ZnO, (b) CdO, (c) GaN, and (d) InN, all in the wurtzite structure, using the LDA (left) and the LDA+ $U$  (right) method. The zero of energy was placed at the valence-band maximum  $E_v$  in each case, i.e., proper band alignments are not included here (see the text).

improvement in the description of the physics of these systems with semicore  $d$  states.

We also should not expect the LDA+ $U$  single-particle energies to agree with photoemission measurements.<sup>42</sup> A comparison with experimental results for the energetic position of the  $d$  states would require a proper analysis of initial and final states, as well as inclusion of self-interaction effects inherent to the LDA. Such a study is not the goal of our present work; we merely point out that, because of these complications, a procedure by which the parameter  $U$  is adjusted in order to reproduce experimental  $d$ -state binding energies is difficult to justify.

Finally, a comment about error bars due to uncertainties in the value of  $U$ : As pointed out in Sec. II, the calculation for  $U^{\text{at}}$  in the case of the Zn atom is carried out with the  $d^9$  configuration as reference configuration, and will tend to overestimate the value of  $U^{\text{at}}$  by  $\sim 1$  eV (as verified in cal-

culations for Cu and Ni atoms). Even an overestimate of 2 eV would only lead to an overestimate of  $\sim 2/3.8 \approx 0.5$  eV after dividing by the dielectric constant of ZnO to obtain the effective  $U$  for the solid. The calculated change in the band gap of ZnO resulting from a modification of  $U$  by this amount is only 0.07 eV. This uncertainty therefore does not affect our main conclusions.

### C. Band lineups

Since the LDA+ $U$  approach systematically improves the LDA band gap, it is interesting to investigate to what extent LDA+ $U$  affects the valence-band maximum and the conduction-band minimum on an absolute energy scale. This question cannot be answered by performing bulk calculations alone, since the long-range nature of the Coulomb potential precludes establishing an absolute reference in a calculation for an infinite solid.<sup>43</sup> The lineup between the band structures obtained in LDA and LDA+ $U$  calculations therefore has to be obtained by following a procedure similar to the calculation of band lineups at semiconductor heterojunctions.<sup>44</sup> We consider ZnO as an example, and calculate the band lineup at the hypothetical  $\text{ZnO}^{\text{LDA}}/\text{ZnO}^{\text{LDA}+U}$  interface, where on one side of the interface ZnO is described by the LDA and on the other side by the LDA+ $U$ . First, we perform calculations for bulk ZnO in the LDA and LDA+ $U$  separately, to determine the valence-band maximum  $E_v$  and the conduction-band minimum  $E_c$  with respect to the respective averaged electrostatic potentials in the bulk solid. Then we align the potentials of the “two materials” by constructing a  $\text{ZnO}^{\text{LDA}}/\text{ZnO}^{\text{LDA}+U}$  superlattice and calculating the averaged electrostatic potential on both sides, in bulk-like regions far from the interface. Since the LDA and the LDA+ $U$  give different lattice constants, we use the average in-plane lattice constant for the superlattice; the resulting hydrostatic strain effect is subtracted out by using the absolute deformation potentials discussed in the next section. To avoid internal electric fields due to the polar nature of ZnO along the  $c$  direction, we construct the superlattice oriented along the nonpolar  $[11\bar{2}0]$  direction. We use an 8+8 superlattice to ensure we have a bulk-like region on both sides of the interface.

The resulting band alignment [Fig. 4(a)] shows the effect of including the on-site Coulomb correlation interaction  $U$  for the Zn  $d$  states. First, it lowers the energy of the Zn  $d$  states with respect to the valence-band maximum; this weakens the  $p$ - $d$  coupling and lowers the valence-band maximum on an absolute energy scale, resulting in a valence-band offset of 0.34 eV between LDA and LDA+ $U$ . The lowering of the valence-band maximum of course results in an increase of the band gap. We note that the increase in the gap (by 0.71 eV) is larger than the amount (0.34 eV) by which the valence-band maximum was lowered, indicating that the LDA+ $U$  has an effect not only on the valence-band maximum but also on the conduction-band minimum. Indeed, Fig. 4 shows that the conduction-band minimum is raised by 0.37 eV. We attribute the change in the conduction band to the following effect: the introduction of  $U$  causes the Zn  $d$  band to become narrower and the Zn  $d$  states to become

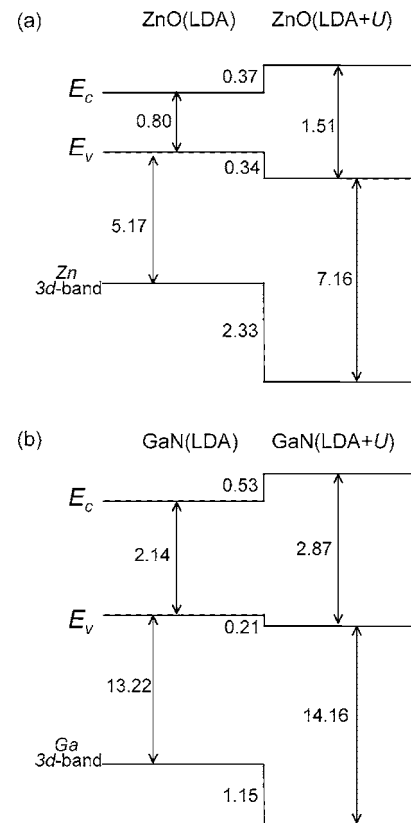


FIG. 4. Calculated band alignment at the hypothetical interfaces (a)  $\text{ZnO}^{\text{LDA}}/\text{ZnO}^{\text{LDA}+U}$  and (b)  $\text{GaN}^{\text{LDA}}/\text{GaN}^{\text{LDA}+U}$  illustrating the effects of including the on-site Coulomb correlation  $U$  for the Zn and Ga  $d$  states.

more localized around the Zn atom. This results in the valence  $4s$  state becoming more effectively screened and thus more delocalized, and therefore its energy increases. Since the states at the conduction-band minimum are composed mainly of Zn  $4s$  states, we observe an increase in the energy of the conduction-band minimum.

In Fig. 4(b) we show the effects of including  $U$  for the Ga  $d$  states on the valence-band maximum and conduction-band minimum of GaN on an absolute energy scale. The effect on the valence-band maximum is smaller than in ZnO, consistent with the larger energy difference between the  $d$  states and the valence-band maximum in GaN.

### D. Absolute deformation potentials

The magnitude of the  $p$ - $d$  coupling increases when the crystal is compressed. Therefore, the LDA+ $U$  correction in the position of the cation  $d$  states with respect to the valence-band maximum is also expected to affect the pressure coefficient (i.e., the deformation potential) of the valence band. The absolute deformation potential, which measures the change in the band energy on an absolute energy scale,<sup>45</sup> is calculated similarly to a heterojunction band offset, by using a superlattice consisting of alternately strained layers of a single material. Details of the procedure are given elsewhere.<sup>8,45,46</sup> Table III lists the calculated absolute deformation potentials for the valence band  $a_v = dE_v/d \ln V$  and for

the conduction band  $a_c = dE_c/d \ln V$ , as well as the band-gap deformation potential  $a_g = a_c - a_v$ . We note that the inclusion of the on-site Coulomb interaction through the LDA+ $U$  method causes the valence-band deformation potential  $a_v$  to increase in value; i.e., it becomes less negative in the case of ZnO, and increases in magnitude in the case of GaN. This is a direct consequence of the weakening of the  $p$ - $d$  coupling in the LDA+ $U$  approach. We note that the value of  $a_g = -7.7$  eV for GaN using the LDA+ $U$  is in better agreement with recent experimental results<sup>47,48</sup> than the LDA value. For CdO and InN, the changes are small. We note that in the case of InN, the band gap is negative ( $\Gamma_1^c$  below  $\Gamma_1^v$ ) at the equilibrium volume and becomes positive ( $\Gamma_1^c$  above  $\Gamma_1^v$ ) when compressed. The repulsion of the  $\Gamma_1^c$  and  $\Gamma_1^v$  states is likely responsible for overestimating  $a_v$  and  $|a_c|$  in the LDA approximation.

#### IV. CONCLUSIONS

We have shown that including on-site Coulomb correlation interactions for the semicore  $d$  states using the LDA+ $U$  method systematically improves the calculated LDA band gap in ZnO, CdO, GaN, and InN. We find that  $U$  affects both the valence-band maximum and the conduction-band minimum. It lowers the energy of the  $d$ -band states, weakening the anion-cation  $p$ - $d$  coupling and lowering the valence-band maximum (which consists mainly of anion  $p$  states). The  $d$  band becomes narrower and the  $d$  electrons become more localized around the cation, thereby delocalizing the cation valence  $s$  states. The latter effect raises the energy of the conduction-band minimum (which consists mainly of cation  $s$  states). These shifts were elucidated by calculating the band alignment between the LDA and LDA+ $U$  band structures. We also investigated the effect of correcting the  $d$ -band positions on deformation potentials. In summary, we find that the LDA+ $U$  treatment produces a specific improvement in the description of the physics of systems with semicore  $d$  states.

Based on this improved description, we have reported electronic band structures for ZnO, GaN, and InN in the

TABLE V. Calculated absolute deformation potentials (in eV) for the valence band  $a_v$ , for the conduction band  $a_c$ , and for the band gap  $a_g$ , for wurtzite ZnO, CdO, GaN, and InN in the LDA and LDA+ $U$  approximations.

	ZnO	CdO	GaN	InN
LDA				
$a_v$	-0.6	-0.1	2.1	1.5
$a_c$	-2.3	0.2	-4.9	-2.7
$a_g$	-1.7	0.3	-7.0	-4.2
LDA+ $U$				
$a_v$	-0.2	0.0	2.3	1.4
$a_c$	-3.1	-0.4	-5.4	-1.7
$a_g$	-2.9	-0.4	-7.7	-3.1

wurtzite phase, and for MgO and CdO in both the wurtzite and rocksalt phases. Based on our calculations we predict a value of 0.92 eV for the direct band gap of CdO (Table IV). We also reported effects on the band offsets (Fig. 4) and on the deformation potentials that describe the variation of band edges under pressure (Table V). Since MgO and CdO occur naturally in the rocksalt phase, no experimental data are available that would allow deriving values for wurtzite-phase MgZnO and CdZnO alloys by interpolation; our predicted results for structural and electronic properties will therefore be useful for deriving such alloy properties.

#### ACKNOWLEDGMENTS

This work was supported by AFOSR under Contract No. F49620-02-1-1163, through a subcontract from the Palo Alto Research Center Incorporated; by ONR under Contract No. N00014-02-C-0433; by the MRSEC Program of the National Science Foundation under Award No. DMR05-20415; and by CNSI-UCSB computing facility. We thank C. Ederer, N. Spaldin, R. Janisch, P. Gopal (UCSB), and L. Petit (ORNL) for helpful discussions.

<sup>1</sup>T. Makino, C. H. Chia, N. T. Tuan, H. D. Sun, Y. Segawa, M. Kawasaki, A. Ohtomo, K. Tamura, and H. Koinuma, Appl. Phys. Lett. **77**, 975 (2000).

<sup>2</sup>A. Ohtomo, M. Kawasaki, T. Koida, K. Masubuchi, H. Koinuma, Y. Sakurai, Y. Yoshida, T. Yasuda, and Y. Segawa, Appl. Phys. Lett. **72**, 2466 (1998).

<sup>3</sup>H. D. Sun, T. Makino, N. T. Tuan, Y. Segawa, M. Kawasaki, A. Ohtomo, K. Tamura, and H. Koinuma, Appl. Phys. Lett. **78**, 2464 (2001).

<sup>4</sup>T. Makino, Y. Segawa, M. Kawasaki, A. Ohtomo, R. Shiroki, K. Tamura, T. Yasuda, and H. Koinuma, Appl. Phys. Lett. **78**, 1237 (2001).

<sup>5</sup>A. Mang, K. Riemann, and S. Rubenacke, Solid State Commun. **94**, 251 (1995).

<sup>6</sup>*Semiconductors-Basic Data*, 2nd revised ed., edited by O. Madelung (Springer, Berlin, 1996).

<sup>7</sup>S. H. Wei and A. Zunger, Phys. Rev. B **37**, 8958 (1988).

<sup>8</sup>C. G. Van de Walle and J. Neugebauer, Appl. Phys. Lett. **70**, 2577 (1997).

<sup>9</sup>P. Hohenberg and W. Kohn, Phys. Rev. **136**, B864 (1964); W. Kohn and L. J. Sham, Phys. Rev. **140**, A1133 (1965).

<sup>10</sup>J. P. Perdew, R. G. Parr, M. Levy, and J. L. Balduz, Phys. Rev. Lett. **49**, 1691 (1982).

<sup>11</sup>J. P. Perdew, M. Levy, and J. L. Balduz, Phys. Rev. Lett. **51**, 1884 (1983).

<sup>12</sup>L. J. Sham and M. Schlüter, Phys. Rev. Lett. **51**, 1888 (1983).

<sup>13</sup>C. Stampfl and C. G. Van de Walle, Phys. Rev. B **59**, 5521 (1999).

<sup>14</sup>P. Rinke, A. Qteish, J. Neugebauer, C. Freysoldt, and M. Scheffler, New J. Phys. **7**, 126 (2005).



- <sup>15</sup>S. Massidda, R. Resta, M. Posternak, and A. Baldereschi, Phys. Rev. B **52**, 16977 (1995).
- <sup>16</sup>P. Schröder, P. Krüger, and J. Pollmann, Phys. Rev. B **47**, 6971 (1993).
- <sup>17</sup>W. R. L. Lambrecht, B. Segal, S. Strite, G. Martin, A. Agarwal, H. Morko, and A. Rockett, Phys. Rev. B **50**, 14155 (1994).
- <sup>18</sup>V. I. Anisimov, J. Zaanen, and O. K. Andersen, Phys. Rev. B **44**, 943 (1991).
- <sup>19</sup>V. I. Anisimov, I. V. Solovyev, M. A. Korotin, M. T. Czyzyk, and G. A. Sawatzky, Phys. Rev. B **48**, 16929 (1993).
- <sup>20</sup>A. I. Liechtenstein, V. I. Anisimov, and J. Zaanen, Phys. Rev. B **52**, R5467 (1995).
- <sup>21</sup>V. I. Anisimov, F. Aryasetiawan, and A. I. Liechtenstein, J. Phys.: Condens. Matter **9**, 767 (1997).
- <sup>22</sup>G. K. H. Madsen and P. Novak, Europhys. Lett. **69**, 777 (2005).
- <sup>23</sup>M. Cococcioni and S. Gironcoli, Phys. Rev. B **70**, 235121 (2005).
- <sup>24</sup>C. Persson and A. Zunger, Phys. Rev. B **68**, 073205 (2003).
- <sup>25</sup>G. Kresse and J. Furthmüller, Phys. Rev. B **54**, 11169 (1996); G. Kresse and J. Furthmüller, Comput. Mater. Sci. **6**, 15 (1996).
- <sup>26</sup>P. E. Blöchl, Phys. Rev. B **50**, 17953 (1994). G. Kresse, and J. Joubert, *ibid.* **59**, 1758 (1999).
- <sup>27</sup>O. Bengone, M. Alouani, P. Blöchl, and J. Hugel, Phys. Rev. B **62**, 16392 (2000).
- <sup>28</sup>J. P. Perdew and A. Zunger, Phys. Rev. B **23**, 5048 (1981).
- <sup>29</sup>W. M. Temmerman, A. Svane, Z. Szotek, and H. Winter, in *Electronic Density Functional Theory: Recent Progress and New Directions*, edited by J. F. Dobson, G. Vignale, and M. P. Das (Plenum, New York, 1998), p. 327.
- <sup>30</sup>P. Giannozzi, S. de Gironcoli, P. Pavoni, and S. Baroni, Phys. Rev. B **43**, 7231 (1991).
- <sup>31</sup>X. Gonze, J.-M. Beuken, R. Caracas, F. Detraux, M. Fuchs, G.-M. Rignanese, L. Sindic, M. Verstraete, G. Zerah, F. Jollet, M. Torrent, A. Roy, M. Mikami, Ph. Ghosez, J.-Y. Raty, and D. C. Allan, Comput. Mater. Sci. **25**, 478 (2002); X. Gonze, Phys. Rev. B **55**, 10337 (1997); X. Gonze and C. Lee, *ibid.* **55**, 10355 (1997).
- <sup>32</sup>M. S. Hybertsen and S. G. Louie, Phys. Rev. B **34**, 5390 (1986).
- <sup>33</sup>Z. H. Levine and D. C. Allan, Phys. Rev. Lett. **63**, 1719 (1989); X. Gonze, Ph. Ghosez, and R. W. Godby, *ibid.* **74**, 4035 (1995).
- <sup>34</sup>*Handbook of Chemistry and Physics*, 46th ed., edited by R. C. Weast (The Chemical Rubber Co., Cleveland, 1965).
- <sup>35</sup>J. A. Van Vechten, Phys. Rev. **182**, 891 (1969).
- <sup>36</sup>W. R. L. Lambrecht, S. Limpijumngong, and B. Segall, MRS Internet J. Nitride Semicond. Res. **4S1**, G6.8 (1999).
- <sup>37</sup>S. Limpijumngong and W. R. L. Lambrecht, Phys. Rev. B **63**, 104103 (2001).
- <sup>38</sup>H. Schulz and K. H. Thiemann, Solid State Commun. **23**, 815 (1977).
- <sup>39</sup>C. McGuinness, C. B. Stagaescu, P. J. Ryan, J. E. Downes, D. Fu, K. E. Smith, and R. G. Egdell, Phys. Rev. B **68**, 165104 (2003).
- <sup>40</sup>X. Li, D. L. Young, H. Moutinho, Y. Yan, C. Narayanswamy, T. A. Gessert, and T. J. Coutts, Electrochem. Solid-State Lett. **4**, C43 (2001).
- <sup>41</sup>J. Wu, W. Walukiewicz, K. M. Yu, J. W. Arger III, E. E. Haller, H. Lu, W. J. Schaff, Y. Saito, and Y. Nanishi, Appl. Phys. Lett. **80**, 3967 (2002).
- <sup>42</sup>R. T. Girard, O. Tjernberg, G. Chiaia, S. Söderholm, U. O. Karlsson, C. Wigren, H. Nylén, and I. Lindau, Surf. Sci. **373**, 409 (1997).
- <sup>43</sup>L. Kleinman, Phys. Rev. B **24**, 7412 (1981).
- <sup>44</sup>C. G. Van de Walle and R. M. Martin, Phys. Rev. B **35**, 8154 (1987).
- <sup>45</sup>C. G. Van de Walle and R. M. Martin, Phys. Rev. Lett. **62**, 2028 (1989).
- <sup>46</sup>A. Janotti and C. G. Van de Walle (unpublished).
- <sup>47</sup>W. Shan, W. Walukiewicz, E. E. Haller, B. D. Little, J. J. Song, M. D. McCluskey, N. M. Johnson, Z. C. Feng, M. Schurman, and R. A. Stall, J. Appl. Phys. **84**, 4452 (1998).
- <sup>48</sup>S. X. Li, J. Wu, E. E. Haller, W. Walukiewicz, W. Shan, H. Lu, and W. J. Schaff, Appl. Phys. Lett. **83**, 4963 (2003).